

SIMULATION OF A GALLIUM ARSENIDE RUNNING WAVE AMPLIFIER WITH A SCHOTTKY BARRIER BY THE MONTE CARLO METHOD

A. Jelenski, I. E. Tralle, and
V. A. Sizyuk

UDC 621.382

Process of transfer of electrons in a gallium arsenide running-wave amplifier with a Schottky barrier has been investigated. Simulation of the process has been implemented by the Monte Carlo method with the use of the three-valley ($\Gamma L X$) model of the GaAs conduction band with account for the nonparabolicity of the bands, scattering on phonons, and transport between valleys. The increment of spatial-charge wave (SCW) has been calculated; it has been shown that the amplification in such a device can be substantially greater than in a beam-instability amplifier.

Introduction. Advancing into the area of millimeter and submillimeter waves and striving for further miniaturization and integration of functions of elements within a single monolithic circuit are the main tendencies in the development of superhigh-frequency solid-state electronics. Precisely this and a number of other considerations [1, 2] produce great interest in designing and investigating HHT devices containing active elements with distributed parameters.

Nowadays an active search for the possibilities of amplifying electromagnetic waves in distributed structures on the basis of n -GaAs-type semiconductors with transport of electrons between valleys [3] along with works in the field of creating HHT amplifiers on Gunn diodes is being conducted. Two basic types of amplifiers on such structures, which differ by orientation of the wave vector k relative to the drift of the carriers v_0 [4], are known. Proximity of the phase velocity of the wave of the carriers to the drift velocity is the characteristic property for structures with lengthwise drift (when $v_0 \parallel k$). In structures with transverse drift, when $v_0 \perp k$, propagation of a wave takes place with a velocity close to the speed of light in the medium, and the effect of amplification of an electromagnetic wave is seen in the case of coincidence of the transverse component of the electric field with the direction of the drift of the carriers in a semiconductor with negative differential conductivity.

Lengthwise-drift devices based of the effects of amplification of waves of the spatial charge are of greatest practical interest nowadays. Devices of this type transform the electromagnetic wave of the spatial charge into a spatial-charge wave that propagates in the direction parallel to the constant electric field, amplify it, and then transform it back into an electromagnetic wave. Such structures in the most cases are planar wave-conducting devices on gallium arsenide with a decelerating structure of one or another configuration and a cathode section in the form of a Schottky barrier whose injection coefficient can be controlled.

Until recently, simulation of a spatial-charge running-wave amplifier was limited mostly to investigation of propagation of waves in a flat waveguide with drift of the carriers [4-6]. Incidentally a full analysis of the functioning of such a device and its optimization are impossible without sophisticated treatment of the mechanism of injection of electrons from the Schottky barrier and evolution of the beam during interaction with the spatial-charge wave. Precisely this constitutes the subject matter of this work.

Model and Basic Relations. As was shown in a number of our works [7, 8], during injection of electrons from the quantum well, amplification of spatial-charge waves can be produced due to beam instability that occurs in a 3D semiconducting plasma or in a 2D electron gas. Since the velocities of the injected electrons in such devices

Institute of Technology of Materials of Electronic Technology, Warsaw; Institute of Physics and Technology, National Academy of Sciences of Belarus, Minsk, Belarus. Translated from *Inzhenerno-Fizicheskii Zhurnal*, Vol. 71, No. 5, pp. 891-898, September-October, 1998. Original article submitted May 26, 1997.

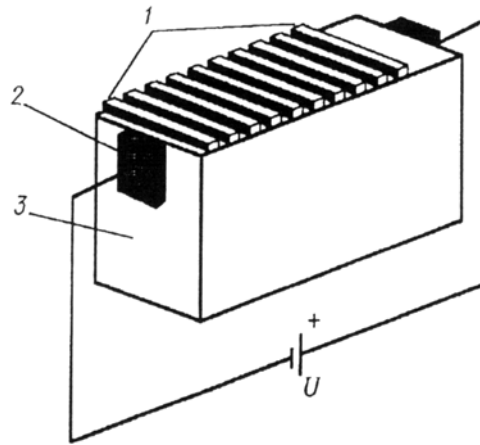


Fig. 1. Schematic representation of the device: 1) grating, 2) Ti contact, 3) gallium arsenide crystal.

are about one order of magnitude greater than the drift velocities of electrons in a semiconductor crystal, the range of oscillations being amplified lies in the area of several hundreds of gigahertz. But as a result of the intense scattering that occurs in a semiconductor, such a beam, as our calculation has shown, penetrates its depth a short distance of 10^{-5} cm, which makes it impossible to reach greater amplification coefficients. Nevertheless, the distribution function of the electrons after "resolution" of the beam finds itself shifted relative to the Maxwell distribution, making it possible to obtain an amplification effect similar to the beam-instability effect at frequencies that are an order of magnitude less by virtue of the fact that the drift velocities of the electrons are less than the initial value of the velocity of the electrons being injected. Amplifiers that work on this principle are called the running-wave amplifiers. Being exceeded in frequency by beam-instability amplifiers, they have at the same time a number of advantages.

It is known that as the requirements imposed by extending the frequency band used for information transmission become more stringent, and as radar technology progresses, the need for high-frequency devices with a small capacitance between the electrodes grows. Designers of the devices are able to resolve the problem by increasing the distance between the electrodes. In avalanche diodes (AD) and Gunn diodes these distances may be increased as long as the time of flight of an electron from the cathode to the anode remains approximately equal to the period of the working oscillation. For precisely this reason both AD and Gunn diodes are able to operate successfully up to frequencies of about 100 GHz. But, since these devices are diodes, their operating characteristics depend on the layout to a very great extent. A running-wave amplifier may be designed in such a way [3] that it would resemble a double-cavity klystron by its internal connections of input and output, and use of a spatial-charge wave that runs between the cathode and the anode makes it possible to obtain a time of flight between the cathode and the anode that is many times greater than the period of the signal. The spatial-charge wave may grow severalfold, but not even this is the main advantage of this amplifier; the main advantage is the increased distance run by the wave, since with a large distance the capacitance between the input and the output is low, which is necessary to ensure stability and wide-bandness of the amplifier.

Thus, we have the microstructure represented schematically in Fig. 1. The grating in it can be created by methods similar to the ones suggested in [9]. Falling on the grating from outside, the microwave field produces a spatial-charge wave, with wave number k equal to the grating's wave number $2\pi/l$, in the semiconductor layer of the structure considered. If the velocity distribution of the particles in the phase-velocity region of the wave turns out to be an increasing function, the Landau damping for this wave gives way to amplification. The mechanism of the latter is the same here as in the case of beam instability: the running wave results in redistribution of electrons in space in such a way that areas with increased concentration of them appear. If this spatial charge is forced to move under an applied external field in the direction of the wave with a velocity greater than the phase velocity of the latter, it will radiate similar to free electrons. Here, amplification is caused by resonance exchange of energy between the wave and the particles, which results in growth of the wave amplitude due to the condition $(df/dv)_{v=\omega/k} > 0$.

A source of electrons that creates beams with a density of the particles comparable to the density of the semiconductor's plasma is a sufficiently effective injector. This can be reached only if the Schottky barrier is narrow enough. As is known [10], the potential barrier is narrowed when the semiconductor is highly alloyed; here a narrow, for the width of the spatial charge, portion adjacent to the electrode [11] is enough to allow for narrowing of the potential barrier between the metal and the semiconductor.

We approximated the shape of the potential barrier in accordance with [10] with account for image forces:

$$\varphi(x) = (\varphi_0 - eU) \left(1 - \frac{x}{L}\right)^2 - \frac{e^2}{4\epsilon_s x} + eU + \mu_s.$$

The width of the Schottky layer is defined by the relation [10]

$$L = \left(\frac{\epsilon_s (\varphi_0 - eU)}{2\pi e^2 n_{\text{con}}} \right)^{1/2}.$$

In subsequent calculations the external voltage imposed on the Schottky layer was taken rather large, but not the breakdown, and equal to 1 V. The equilibrium concentrations of electrons within the region adjacent to the electrode n_{con} and in the volume of the semiconductor n_s were, respectively, 10^{20} and 10^{17} cm^{-3} , and the temperature $T = 300 \text{ K}$. The value μ_s of the Fermi level, calculated by the Shockley method, with these values of the parameters equals to 0.05 eV, $L = 5.1 \cdot 10^{-7} \text{ cm}$, and ϵ_s of gallium arsenide is 13.5.

For the considered injector to be effective, the height of the potential barrier on the metal-dielectric boundary and the work function of the metal must be minimum. Among the least exotic metals titanium satisfies these conditions. The work function and the height of the potential barrier for it amount to 3.83 and 0.74 eV, respectively [13]. Then, the position of the Fermi level in titanium is given by the following relations:

$$\mathcal{E}_F = \mathcal{E}_{F0} \left[1 - \frac{\pi^2}{12} \left(\frac{k_B T}{\mathcal{E}_{F0}} \right)^2 \right], \quad \mathcal{E}_{F0} = \frac{\hbar^2}{2\pi} \left(\frac{3}{8\pi} n_m \right)^{2/3}, \quad n_m = N_A \frac{\rho_m}{M}$$

and it amounts to a value of 5.3 eV with a concentration of electrons in the metal of $5.66 \cdot 10^{22} \text{ cm}^{-3}$.

With account for image forces the height of the Schottky potential barrier calculated relative to the zero energy in titanium (5.37 eV less than the Fermi level of Ti) amounts to 5.89 eV at maximum.

The initial energy distribution of electrons in the metal is defined by the relation [14]

$$dn(\mathcal{E}) = \frac{2\pi}{h^3} (2m_d^*)^{3/2} \frac{\sqrt{\mathcal{E}}}{1 + \exp\left(\frac{\mathcal{E} - \mathcal{E}_F}{k_B T}\right)} d\mathcal{E}. \quad (1)$$

To calculate probabilities of tunneling of electrons through the potential barrier, the WKB approximation was used [15]:

$$D(\mathcal{E}) = \exp\left(-\frac{2}{h} \int_{x_1}^{x_2} \sqrt{2m^* (\Psi - \mathcal{E}_x)} dx\right). \quad (2)$$

However in the case where the particle has an energy greater than the barrier, it is more convenient to use the following formula instead of relation (2):

$$D(\mathcal{E}) = 1 - \frac{k_e^2 (b-a)^2 + (k_e^2 - ab)^2 \tan^2 \varphi}{k_e^2 (b+a)^2 + (k_e^2 + ab)^2 \tan^2 \varphi}.$$

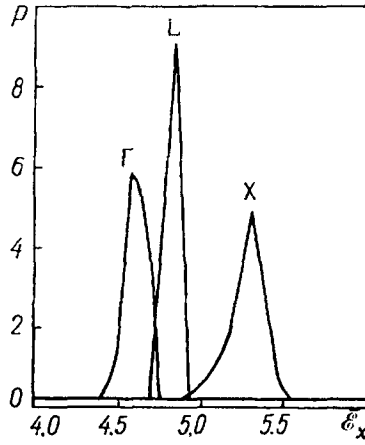


Fig. 2. ε_x -distribution of electrons of a beam for the three valleys in a GaAs crystal immediately after tunneling through the Schottky barrier from Ti. P , arbitrary units; ε_x , eV.

Here the initial wave vector of the particle is $k_e = 1/h(\sqrt{2m^* \varepsilon_x})$, a and b are the lengths of the wave vectors of the particles at the dividing lines of the barrier, in our case:

$$a = k, \quad b = \frac{1}{h} \sqrt{2m^* (\varepsilon_x - \Psi_b)}; \quad \varphi = \frac{1}{h} \int_0^L \sqrt{2m^* (\varepsilon_x - \Psi(x))} dx.$$

Moreover, the influence of the potential step produced by the bottom of the conduction band in the semiconductor has been taken in consideration in the calculation of probabilities of tunneling through the Schottky barrier [16]. For ε_x above the bottom of the conduction band

$$D(\varepsilon) = \left(\frac{k_e - b}{k_e + b} \right)^2.$$

In simulation of processes of transfer of charge in gallium arsenide we used the three-valley (Γ LX) model of its conduction band. In accordance with this model three types of valleys were taken in consideration in the calculation: Γ , L, and X, the gaps between the valleys were $\Delta_{\Gamma L} = 0.31$ eV, $\Delta_{\Gamma X} = 0.48$ eV, and the effective masses were $m_{\Gamma} = 0.067m_0$, $m_L^* = 0.23m_0$, $m_X^* = 0.43m_0$ [17]. As was already shown above, only some of the energy related to the motion of the electron toward the barrier is taken into consideration in tunneling through the Schottky potential barrier. As a result of the greater mass of electrons in the X- and L-valleys, and because these "heavy" valleys form from several equivalent ones, the density of states in the conduction band of GaAs increases sharply from the lower Γ -valley to the upper X-valley. Therefore it was assumed that the overwhelming majority of electrons with energy higher than the gap Δ between the valleys would reach the upper valley.

Thus, we have calculated the energy distributions of, in essence, three "beams" corresponding to the three valleys Γ , L, and X, as a result of which the final output beam of electrons of the injector has gained three corresponding components. The densities of the beam entering the GaAs and of its partial components were found proceeding from the density of electrons in the metal and the ratio between the particles that penetrated the barrier and the particles that are on their way toward it. Calculated distributions are presented in Fig. 2.

As a result of numerical experiments on tunneling through the Schottky barrier of Ti/GaAs, energy distributions of electrons for different directions in the initial beam were obtained in the form of tables (see Fig. 2). The subsequent evolution of the distribution function of electrons during the movement of the beam through the crystal was simulated with the aid of the Monte Carlo method.

As mentioned above, the three-valley model of the conduction band of gallium arsenide was used in the work. The predominance of one or another type of scattering in the semiconductor crystal depends on the possession of the electron by one of the valleys and on the magnitude of the electric field. The electric field in the crystal

considered can be regulated over a wide range by varying the external voltage supplied to the device and the thickness of the semiconducting substrate. Electric fields insufficient for collision ionization (up to 100 kV/cm) were investigated in this work. Under such conditions three types of scattering are the most important in gallium arsenide: on acoustic phonons, on polar optical phonons, and scattering between the valleys [18].

The strong dependence of the probabilities of the chosen types of scattering on the shape of the valleys required account for their nonparabolicity. The coefficients of nonparabolicity of the gallium arsenide valleys were calculated starting from the width of the forbidden zone and amounted to $\alpha_{\Gamma} = 0.645 \text{ eV}^{-1}$, $\alpha_L = 0.538 \text{ eV}^{-1}$, $\alpha_X = 0.493 \text{ eV}^{-1}$.

Description of the interaction between an electron and an acoustical phonon is one of the most complicated and laborious problems in the Monte Carlo simulation, due to the dependence of the direction of the final pulse of the particle on the magnitude and direction of its initial pulse. For the scattering probability with a nonparabolic dispersion law we used the following relation (see [18]):

$$W_{ac}^{\pm}(k_e) = \frac{\Xi_{def}^2 m^*}{4\pi \rho_s s_l \hbar} \frac{1}{\hbar k_e} \int_{q_{min}^{\pm}}^{q_{max}^{\pm}} \left(N_q + \frac{1}{2} \mp \frac{1}{2} \right) q^2 A^{\pm} I_0^{\pm} dq,$$

where the superscript "plus" relates to interaction with absorption of an acoustical phonon, and "minus," with ejection; the longitudinal speed of sound $s_l = 5.2 \cdot 10^5 \text{ cm/sec}$; A^{\pm} , I_0^{\pm} are parameters related to the account for nonparabolicity:

$$A^{\pm} = 1 + 2\alpha (\mathcal{E} \pm \hbar s_l q), \quad I_0^{\pm} = \frac{(1 + 2\alpha \mathcal{E} \pm \alpha \hbar s_l q)^2 - \frac{\alpha \hbar^2 q^2}{2m^*}}{(1 + 2\alpha \mathcal{E}) A^{\pm}}.$$

The following values were used in the calculations for the constants of the deformation potential in each of the three valleys: $\Xi_{def}^{\Gamma} = 7.0 \text{ eV}$ [18], $\Xi_{def}^L = 9.2 \text{ eV}$, $\Xi_{def}^X = 9.3 \text{ eV}$ [19].

The probability of scattering on optical phonons has the form [18]

$$W_{p.o}^{\pm}(k_e) = \frac{e^2 \hbar \omega_{op} m^*}{\hbar^2} \left(\frac{1}{\epsilon_{\infty}} - \frac{1}{\epsilon_s} \right) \left(N_{\omega_{op}} + \frac{1}{2} \mp \frac{1}{2} \right) \frac{1}{\hbar k_e (1 + 2\alpha \mathcal{E})} \times \\ \times \left([1 + 2\alpha \mathcal{E} \pm \alpha \hbar \omega_{op}]^2 \ln \frac{q_{max}^{\pm}}{q_{min}^{\pm}} - \frac{\alpha}{m^*} \hbar^2 k_e k^{\pm} \right).$$

Here

$$N_{\omega_{op}} = \frac{1}{\exp(\hbar \omega_{op}/k_B T) - 1}, \quad q_{min}^{\pm} = \pm (k^{\pm} - k_e), \quad q_{max}^{\pm} = k_e + k^{\pm}, \\ \hbar k^{\pm} = \sqrt{2m_d^* (\mathcal{E} \pm \hbar \omega_{op}) (1 + \alpha [\mathcal{E} \pm \hbar \omega_{op}])},$$

$m_d^* = (m_l m_t^2)^{1/3}$ is the effective mass of the density of states according to Herring–Voigt [20].

Amplification of an SCW. The established velocity distribution of electrons in the crystal with injection of electrons from the Schottky barrier, which we calculated by the Monte Carlo method using the three-valley model of the gallium arsenide conduction band for one of the temperatures, is presented in Fig. 3.

In terms of the Boltzmann distribution law the interaction between the drifting flow of electrons and the running wave can be described by the following system of equations [21, 22]:

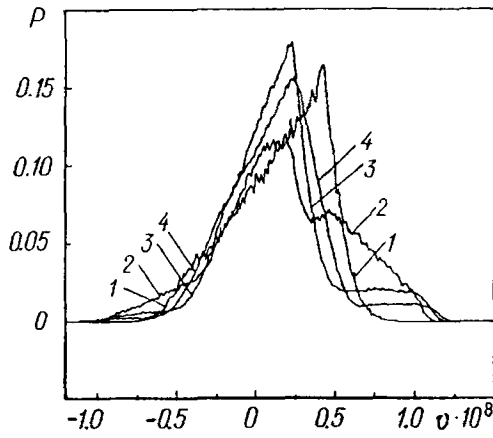


Fig. 3. Velocity distribution of electrons in a drifting beam in GaAs at the temperature $T = 200$ K: 1) $E = 1.5$ kV/cm, 2) 6.0, 3) 15.0, 4) 30.0. v , cm/sec.

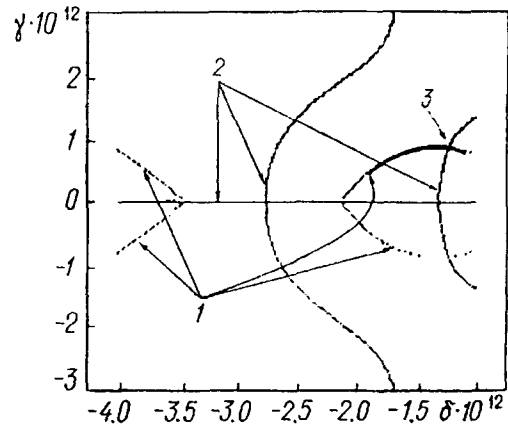


Fig. 4. Graphical solution of the system of equations (4): 1) geometric location of the zeroes of the first equation of system (4), 2) the same for the second equation, 3) region of existence of a positive solution. γ, δ , sec^{-1} .

$$\frac{\partial f_i}{\partial t} + v \frac{\partial f_i}{\partial r} + (r/m_i^*) E \frac{\partial f_i}{\partial v} = -\frac{f_i - f_i^0}{\tau},$$

where f_i^0 , $i = 1, 2$ ($i = 1$ relates to the "shifted" distribution function, $i = 2$ to the "unshifted"), are undisturbed distribution functions without the spatial-charge wave; $m_1^* = m_2^*$.

Dispersion relations for the collective oscillation modes of the "plasma-drifting flow of electrons" system can be obtained using the standard procedure [22, 23] and has the form

$$1 + \frac{4\pi e^2}{\epsilon_s k} \sum_i \int_{-\infty}^{\infty} \frac{\partial f_i^0 / \partial v}{\omega - kv + i\tau_i^{-1}} dv = 0. \quad (3)$$

Let us consider the frequency ω to be a complex quantity and set $\omega = kv_0 + \delta + i\gamma$, where $kv_0 = \omega_0$ and the frequency ω_0 corresponds to the exact phase resonance; δ is the tuning out; $\gamma = \text{Im } \omega + \tau^{-1}$ is the increment. Separating the real and imaginary parts in (3), we arrive at the following system of equations:

$$1 + \frac{4\pi e^2}{\epsilon_s k m^*} \int_{-\infty}^{\infty} \frac{\omega_0 + \delta - kv}{(\omega_0 + \delta - kv)^2 + \gamma^2} \left(\frac{\partial f_1^0}{\partial v} + \frac{\partial f_2^0}{\partial v} \right) dv = 0, \quad (4)$$

$$\int_{-\infty}^{\infty} \frac{\gamma}{(\omega_0 + \delta - kv)^2} \left(\frac{\partial f_1^0}{\partial v} + \frac{\partial f_2^0}{\partial v} \right) dv = 0.$$

For numerical solution of (4) we used the velocity distributions of electrons that resulted from the simulation by the Monte Carlo method (Fig. 3).

Each of Eqs. (4) defines some curve $F_i(\delta, \gamma) = 0$ in the plane (δ, γ) , and, therefore, if the two curves meet at some point P with coordinates (δ', γ') , this pair of numbers satisfies system (4). The numerical solution of (4) is obtained by means of a program that constructs a graph of F_i on the interval $[\delta_{\text{in}}, \delta_{\text{fin}}]$; one more program, which calculates the zeroes of $F_i(\delta, \gamma)$ at the point $\delta \in [\delta_{\text{in}}, \delta_{\text{fin}}]$ on some interval $[\gamma_{\text{in}}, \gamma_{\text{fin}}]$, is used for this. Results of the numerical solution of system (4) are presented in Fig. 4, where curves 1 are zeroes of the first equation, and curves 2 are zeroes of the second equation. The point 3 of their intersection defines the values of the increment and the tuning out, which amount to $\delta = -1.22 \cdot 10^{12} \text{ sec}^{-1}$, $\gamma = 9.0 \cdot 10^{11} \text{ sec}^{-1}$.

The amplification of an SCW is defined by the relation $G = 8.68(\gamma/\omega_0)k_0$. For the grating period $l = 10^{-4}$ cm and the frequency $\omega_0 = 2.76 \cdot 10^{12}$ sec $^{-1}$ this quantity amounted to 4540 dB/mm. The amplification of an electromagnetic wave can be found by a complete electrodynamic analysis of its propagation in the waveguide with the SCW moving in it, which goes beyond this work. But, starting from results of [4], the limiting value of this amplification may be thought of as approximately the number of times less than the indicated value of G that the drift velocity v_0 is less than the speed of light in the medium (in the given case, GaAs), that is, it does not exceed 24 dB/mm.

The work was carried out with financial support of the Foundation for Fundamental Research of the Republic of Belarus, grants No. 006.012 and No. MP96-50.

NOTATION

k , k , wave vector of the spatial-charge wave and its magnitude, respectively; v_0 , drift velocity of electrons in the injected beam; l , grating period; v , v , velocity of electrons in the semiconductor crystal and its magnitude; r , magnitude of the radius vector of the charged particle; f , velocity distribution function of electrons in the semiconductor crystal; ω , cyclic frequency of the spatial charge wave; ω_0 , frequency corresponding to the exact phase resonance; φ_0 , height of the metal-semiconductor potential barrier; U , external voltage; e , charge of the electron; m_0 , mass of the free electron; x , coordinate; L , width of the spatial-charge region; ϵ_∞ and ϵ_s , optical and dielectric permeability of the semiconductor; μ_s , energy gap between the Fermi level in the semiconductor and the bottom of the conduction band; n_{con} , equilibrium concentration of electrons in the alloyed region adjacent to the contact of the semiconductor; n_s , equilibrium concentration of electrons in the volume of the semiconductor; n_m , equilibrium concentration of electrons in the metal; T , temperature; \mathcal{E}_F , Fermi level; \mathcal{E}_{F0} , Fermi level at $T = 0$ K; k_B , Boltzmann constant; N_A , Avogadro number; D , transparency of the potential barrier; $\hbar = h/2\pi$, Planck constant; ρ_m , ρ_s , densities of the metal and the semiconductor, respectively; M , molar mass; m^* , effective mass of the charge carrier in the semiconductor crystal; m_d^* , effective mass of the density of states; m_l , m_t , longitudinal and transverse effective masses; \mathcal{E} , energy of the electron; \mathcal{E}_x , component of the kinetic energy of the electron \mathcal{E} specified by its motion in the x direction; Ψ , potential energy; x_1 , x_2 , classical turning points; k_e , magnitude of the wave vector of the electron; a , b , magnitudes of the wave vectors of the particle at the dividing lines of the barrier; Ψ_b , energy of the conduction band bottom of the semiconductor relative to the zero energy in the metal; $\Delta_{\Gamma L}$, $\Delta_{\Gamma X}$, energy gaps between the valleys; m_Γ^* , m_L^* , m_X^* , effective masses of electrons in the Γ , L, and X valleys, respectively; α_Γ , α_L , and α_X , nonparabolicity coefficients of the Γ , L, and X valleys, respectively; E , E , intensity of the electrical field and its magnitude, respectively; W_{ac} , probability of scattering of an electron on an acoustic phonon; Ξ_{def} , effective constant of the deformation potential; s_l , longitudinal speed of sound; q , wave vector of the interacting phonon; $q_{min/max}$, minimum (maximum) wave vector of the interacting phonon; N_q , the number of thermodynamically equilibrium acoustic phonons; A^\pm , I_0^\pm , coefficients related to the account for nonparabolicity; $\hbar\omega_{op}$, energy of the optical phonon; $N_{\omega_{op}}$, number of thermodynamically equilibrium optical phonons; τ , relaxation time; δ , tuning out from the exact-resonance frequency; γ , increment of the spatial-charge wave; G , amplification of the spatial-charge wave. Abbreviations: ΓLX model, the model of the conduction band of GaAs with account for the Γ , L, and X valleys; SCW, spatial-charge wave; AD, avalanche diode; WKB approximatrion, Wentzel–Kramers–Brillouin approximation. Subscripts: Γ , X, L, the Γ , X, L valleys of the gallium arsenide conduction band, respectively; m, s, metal and semiconductor, respectively; l , t , longitudinal and transverse components; def, deformation; ac, acoustic; p.o, polar optical; op, optical; min, max, minimum and maximum; x , the x coordinate; in, fin, initial and final, respectively; b, bottom of the conduction band.

REFERENCES

1. E. V. Lyubchenko, G. S. Makeeva, and E. I. Nefedov, Radiotekhnika i roman e back 37 up 25 primelektronika, No. 9, 1665-1682 (1982).
2. A. Jelenski, A. Grub, V. Krozer, and H. L. Hartnagel, IEEE Trans. Microw. Th. Tech., 41, No. 4, 549-557 (1993).

3. R. H. Dean and R. J. Matarese, Proc. IEEE, **60**, No. 12, 1486-1506 (1972).
4. A. A. Barybin and V. M. Prigorovskii, Elektron. Tekhn., Ser. Elektron. Sverkhvys. Chast., No. 12, 8-14 (1987).
5. S. N. Tolstolutskiĭ, V. S. Mikhailovskii, and Yu. M. Sinel'nikov, Izv. VUZov, Radiofiz., **30**, 1498-1504 (1987).
6. S. G. Ingram and J. C. Clifton, IEEE Trans. Microw. Th. Tech., **44**, No. 6, 956-960 (1996).
7. I. E. Tralle and V. A. Sizjuk, Phys. Stat. Sol. (b), **182**, 171-176 (1994).
8. I. E. Tralle and V. A. Sizjuk, Phys. Stat. Sol. (b), **186**, 85-94 (1996).
9. S. J. Allen, D. C. Tsui, and F. De Rosa, Phys. Rev. Lett., **35**, 980-983 (1977).
10. V. I. Strikha, Theoretical Foundations of Operation of Metal-Semiconductor Contacts [in Russian], Kiev (1974).
11. R. S. Popovič, Solid-State Electronics, **21**, 1133-1138 (1978).
12. V. Shockley, Theory of Electronic Semiconductors [Russian translation], Moscow (1953).
13. K. Kim, M. Kniffin, R. Sinclair, and C. Helms, J. Vac. Sci. Technol. A, No. 3, Pt. 2, 1473-1477 (1988).
14. V. V. Pasyukov and V. V. Sorokin, Materials of the Electronic Technology [in Russian], Moscow (1986).
15. K. Kao and W. Hwang, Electron Transport in Solids [Russian translation], Moscow (1984).
16. L. D. Landau and E. K. Lifshits, Quantum Mechanics [in Russian], Moscow (1972).
17. B. Ridley, Quantum Processes in Semiconductors [Russian translation], Moscow (1986).
18. V. M. Ivashchenko and V. V. Mitin, Simulation of Kinetic Phenomenons in Semiconductors. The Monte Carlo Method [in Russian], Kiev (1990).
19. K. Brennan and K. Hess, Solid-State Electronics, **27**, No. 4, 347-357 (1984).
20. E. M. Conuell, High-Field Transport in Semiconductors [Russian translation], Moscow (1970).
21. L. A. Artsimovich and R. Z. Sagdeev, Plasma Physics for Physicists [in Russian], Moscow (1979).
22. B. B. Robinson and B. Vural, RCA Rev., **29**, 270-279 (1968).
23. D. Pines and J. R. Schriber, Phys. Rev., **124**, No. 5, 1387-1400 (1961).